Study of Translational and Rotational Mobility and Orientational Preference of Ethane in One-Dimensional Channels

Shreyas Y. Bhide[†,‡] and S. Yashonath*[,†,§,#]

Solid State and Structural Chemistry Unit and Supercomputer Education and Research Centre, Indian Institute of Science, Bangalore-560012, India

Received: January 14, 2002; In Final Form: April 15, 2002

Structural and dynamical properties of ethane in one-dimensional channels of $AlPO_4$-5 and carbon nanotube have been investigated at dilute concentration with the help of molecular dynamics simulation. Density distributions and orientational structure of ethane have been analyzed. Repulsive interactions seem to play an important role when ethane is located in the narrow part of the $AlPO_4$-5 channel. In $AlPO_4$-5, *parallel* orientation is predominant over *perpendicular* orientation except when ethane is located in the broader part of the channel. Unlike in the case of single-file diffusion, our results in carbon nanotube show that at dilute concentrations the mean squared displacement, $u^2(t) \approx t^\alpha$, $\alpha = 1.8$. The autocorrelation function for the *z*-component of angular velocity of ethane in space-fixed frame of reference shows a pronounced negative correlation. This is attributed to the restriction in the movement of ethane along the *x*- and *y*- directions. It is seen that the ratio of reorientational correlation times does not follow the Debye model for confined ethane but it is closer to the predictions of the Debye model for bulk ethane.

1. Introduction

In recent years, there has been an increasing interest in studying properties of confined fluids in microporous solids.[1,2] In particular, there have been many studies directed toward understanding properties of hydrocarbons in zeolites.[3,4] This is primarily due to the importance of zeolites in the petrochemical industry for cracking of long-chain hydrocarbons and separation of mixtures. In both of these processes, mobility of molecules inside the microporous host plays a crucial role. This necessitates a study of the influence of confinement on self-diffusivity of molecules.

In the case of polyatomic molecules, in addition to translational degrees of freedom, rotational motion is also present. This prompts some questions: In what manner does the rotational diffusivity of a molecule change in confinement? How does the translational motion of a molecule get affected by its rotational motion in confinement? Answers to these questions can give a better understanding about mobility of polyatomic molecules in confinement. This in turn can help in designing of better separation, as well as catalytic, processes.

To answer the above-mentioned and related questions, we have studied ethane in one-dimensional channels. While ethane represents one of the simplest of the polyatomic molecules, namely, a linear molecule composed of two CH_3 groups, one-dimensional channels represent the simplest topology of interconnected pores, which are devoid of complications associated with higher-dimensional channels. One-dimensional channel systems explored in the present study are $AlPO_4$-5 and carbon nanotube. These have varying degrees of surface roughness and modulation of channel diameter along the channel: $AlPO_4$-5 has *rough* or *structured* channel walls and it also shows modulation in diameter along the channel. As opposed to this, the wall of carbon nanotube is *smooth* or *structureless* and it has a constant diameter throughout.

Adsorption and dynamical properties of ethane in one-dimensional channels of $AlPO_4$-5 and carbon nanotube have been studied earlier experimentally, as well as by computer simulations. Recent molecular dynamics (MD) simulations of ethane in carbon nanotube and $AlPO_4$-5 address different aspects of ethane motion. Demontis and co-workers[5] found no evidence for concerted diffusion of an ethane cluster inside a flexible framework of $AlPO_4$-5, and their study ruled out any single-file behavior of ethane inside $AlPO_4$-5. A method of calculation of minimum free energy paths has been used by Sholl[6] to characterize passage of ethane molecules inside $AlPO_4$-5. A MD study of Mao and Sinnott[7] found that the nature of diffusive motion of ethane in carbon nanotube changes with the diameter of the nanotube. Experimentally, the dynamics of ethane in $AlPO_4$-5 has been studied by quasi-elastic neutron scattering (QENS)[8] and pulsed-field gradient (PFG) NMR measurement.[9] The heat of adsorption of ethane in $AlPO_4$-5 has been determined by the gas chromatography pulse technique[10] and by adsorption calorimetry.[11] Ethane adsorption isotherms have been studied by the grand canonical Monte Carlo (GCMC) method.[12] More references to earlier simulation and experimental studies of ethane can be found in ref 5.

In the above-mentioned simulation and experimental studies, the properties of ethane are influenced by intermolecular interactions, in addition to the interactions of ethane with the host atoms. As opposed to these earlier studies, the present work aims at studying the effect of confinement alone on the energetics and dynamics of ethane in the dilute limit. Choosing a dilute concentration helps us to clearly distinguish the effect of confinement from effects due to other factors.

* To whom correspondence should be addressed. E-mail: yashonath@sscu.iisc.ernet.in.

† Solid State and Structural Chemistry Unit.

‡ E-mail: bhide@sscu.iisc.ernet.in.

Also at Condensed Matter Theory Unit, Jawaharlal Nehru Centre for Advanced Scientific Research.

§ Supercomputer Education and Research Centre.

10.1021/jp020101e CCC: $22.00
Published on Web 07/12/2002

2. Structure of Hosts

The two structures, namely, (i) $AlPO_4$-5 and (ii) carbon nanotube, have one-dimensional channels along the *c* axis. $AlPO_4$-5 crystallizes in hexagonal space group *P*6/*mcc* with $a = 13.77$ and $c = 8.38$ Å.[13] There are 72 atoms in one unit cell. The channel does not have uniform diameter throughout (Figure 1a,b); it is narrower near $z \approx 0.25c$ and $0.75c$ (diam $\approx$ 10.02 Å) but broader in the rest of the region (diam $\approx$ 11.37 Å).

The carbon nanotube structure is constructed by the method of arm-chair mode of rolling the graphite sheet[14,15] (see Figure 1c). It is possible to have carbon nanotube with different diameters. Here, we have chosen an (8,8) single-walled carbon nanotube. The length of a single carbon nanotube is taken to be $c = 49.29$ Å, which contains 640 carbon atoms. Unlike $AlPO_4$-5, the carbon nanotube has uniform diameter, and the wall is smooth and homogeneous throughout. Thus, these one-dimensional channels represent structures with different degrees of undulations in channel diameters and differences in surface roughness and homogeneity of channel walls.

3. Intermolecular Potential

Ethane is considered as a diatomic molecule within the united atom model approximation. Lennard-Jones potential is employed for sorbate−sorbate and sorbate−host interactions,

$$\phi_{ij}(r_{ij}) = -\frac{A_{ij}}{r_{ij}^{6}} + \frac{B_{ij}}{r_{ij}^{12}} \qquad (1)$$

The potential parameters, $A_{ij} = 4\epsilon_{ij}\sigma_{ij}^{6}$ and $B_{ij} = 4\epsilon_{ij}\sigma_{ij}^{12}$, for sorbate−sorbate interaction are taken from Jorgensen et al.[16] The parameters for sorbate−host interactions can be obtained from Lorentz−Berthelot combination rules once the interaction parameters of host atoms are known. Ethane is assumed to interact only with oxygen atoms of $AlPO_4$-5. The parameters for oxygen have been taken from earlier work on adsorption of hydrocarbons in zeolites and aluminophosphates.[17,18] It will be seen that these parameters are able to reproduce the experimental value of ΔH_{ads}. In the case of carbon nanotube, no experimental data on ΔH_{ads} for ethane is available. We have therefore chosen the C−C parameters of Steele.[19] These have been used subsequently, among others, by Ayappa[14] for study of binary mixtures in carbon nanotubes and by Zhang[15] for simulation of linear alkanes in carbon nanotubes. These parameters are listed in Table 1.

4. Computational Details

All molecular dynamics (MD) simulations have been carried out in the microcanonical ensemble (NVE) with cubic periodic boundary conditions. The system consists of $16 \times 16 \times 6$ unit cells in the case of $AlPO_4$-5, which makes in all 256 channels along the *c* direction with each channel being six unit cells long. In the case of carbon nanotube, 256 tubes are arranged in a hexagonal fashion with all tubes parallel to the *c* direction. In the plane perpendicular to the *c* axis, two channel centers are separated by a distance of 14.28 Å. Two ethane molecules reside in each channel, which corresponds to a total of 512 molecules in each host. This corresponds to a concentration of 0.33 ethane molecules per unit cell in $AlPO_4$-5 and 0.04 ethane molecules per angstrom in carbon nanotube. Because ethane−ethane interaction is minimal, the role of the ethane−host interaction is dominant. The spherical cutoff radius, r_c, measured from the center of mass of ethane for both ethane−ethane and ethane−host interaction is taken to be 12 Å. Thus, a given ethane molecule interacts with molecules and host atoms in neighboring channels as well. For bulk ethane, calculations are carried out at a density of 0.544 g/cm^3 for a total of 108 molecules. This density corresponds to the bulk liquid density of ethane,[16] which is higher than the density of ethane considered in $AlPO_4$-5 (0.038 g/cm^3) and carbon nanotube (0.046 g/cm^3) in the present study.

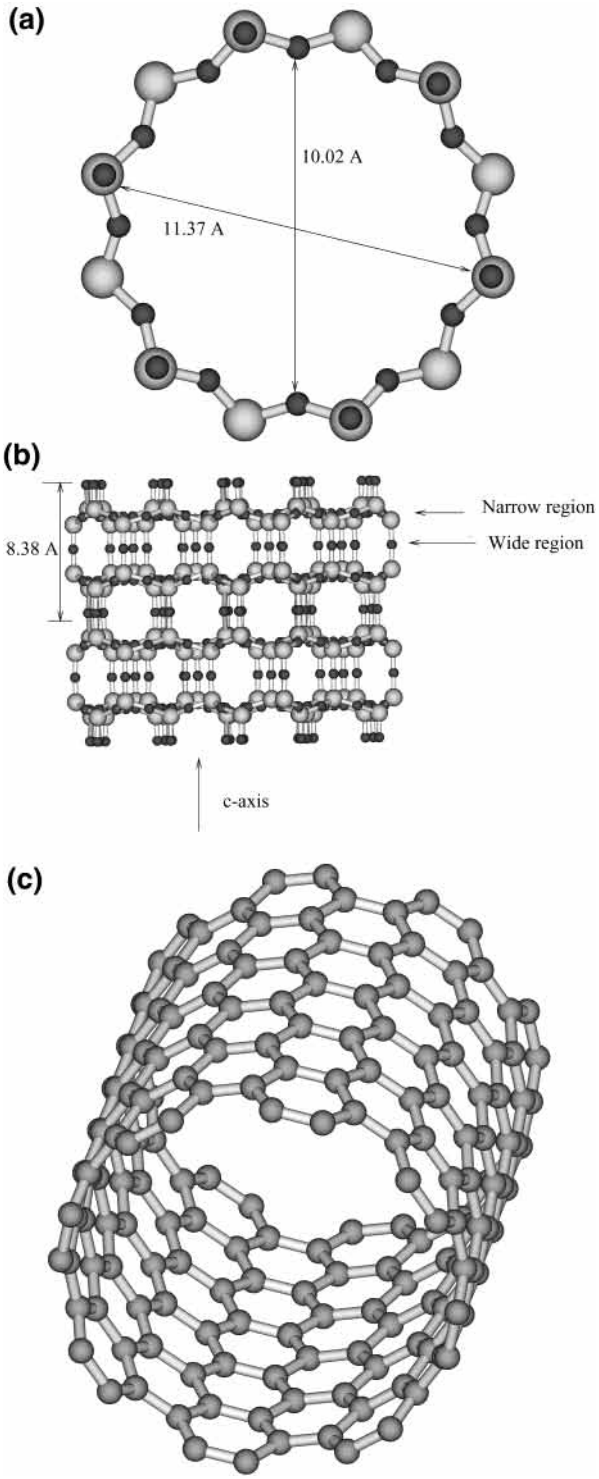

Figure 1. Schematic view of different hosts and their channel diameters. For $AlPO_4$-5 dark spheres correspond to oxygens. Panel a shows a cross-sectional view of the $AlPO_4$-5 channel. There are two diameters, the narrow (10.02 Å) and the broad (11.37 Å), which correspond, respectively, to the 12-ring window plane and region connecting two such window planes. Panel b shows a vertical view of the $AlPO_4$-5 channel with the different regions indicated along the channel. Panel c shows a carbon nanotube.

TABLE 1: Lennard-Jones Potential Parameters

	σ (Å)	ϵ (kJ/mol)
CH_3-CH_3	3.775	0.8660
	$AlPO_4$-5	
O−O	2.529	1.51
	carbon nanotube	
C_n-C_n	3.4	0.2328

The spherical cut off radius is taken to be $r_c = 11$ Å for bulk ethane calculations.

The Gear predictor−corrector algorithm[20] is used for integration of translational and rotational equations of motion for ethane molecules. The host structure is kept rigid. A time step of 1 fs has been used. This gives conservation in total energy of 5 in 10^5. Different properties are calculated using positions and velocities stored every 20 fs. The system is equilibrated for 100 ps in each case. At the beginning of the equilibration phase, ethane molecules are put at the center of the channel with initial velocities chosen randomly from a uniform distribution. This is followed by a production run of 150 ps. All runs have been carried out at a temperature of 200 K.

For the ethane molecule, the bond length, l, between CH_3 groups is taken to be 1.53 Å. The mass of the CH_3 group is taken to be 15.034 amu.

5. Results and Discussion

In recent MD investigations of benzene,[21] a planar molecule, and methane,[18] a globular molecule having tetrahedral shape, diffusing within the one-dimensional channels of $AlPO_4$-5 and carbon nanotube, it was found that the orientation and its rotational motion were drastically affected by confinement. In the case of benzene, for example, anisotropy in rotational motion inside one-dimensional channels is not what one expects from its molecular geometry. Methane exhibited strong inclination toward scissors or 2 + 2 orientation with respect to the channel axis as opposed to inverted umbrella or 1 + 3 orientation. Ethane is a linear molecule of which the equilibrium structural—positional as well as orientational—properties and dynamical—translational as well as rotational—motion are investigated here.

5.1. Energetics and Structure. Figure 2a shows the average ethane−host interaction energy $\langle U_{gh}\rangle$ as a function of the z coordinate of the center of mass of ethane along the c axis. Note that in all figures, z is shown scaled by c. In $AlPO_4$-5, $\langle U_{gh}\rangle$ at $z/c = 0.25$ and 0.75 is higher by ~4 kJ/mol as compared to $\langle U_{gh}\rangle$ values at the wider parts of the channel. These positions correspond to a constriction of the channel. In carbon nanotube, there are no significant variations in $\langle U_{gh}\rangle$ as a function of z. In general, careful analyses of Derouane and co-workers[22] showed that for a molecule of a given size, its attractive interaction with the host increases as the pore dimension becomes smaller or as the curvature increases. This suggests that $\langle U_{gh}\rangle$ should be greater in magnitude in the narrow part of the $AlPO_4$-5 channel than in the wider part of the channel. But, Figure 2a shows the opposite: the wider part interacts more strongly with ethane. This is because a decrease in void size beyond the sorbate size leads to overlap of electron clouds of the guest and the host zeolite, which causes repulsive interaction. As a result, the magnitude of $\langle U_{gh}\rangle$ decreases with a decrease in void size. This implies that in the narrow part of the channel in $AlPO_4$-5 the repulsive part of the potential contributes more to $\langle U_{gh}\rangle$ than in wider part of the channel.

Figure 2b shows a plot of $\langle U_{gh}\rangle$ as a function of r, the radial distance of the center of mass of ethane from the channel axis. r is scaled by R, the radius of the respective channel defined as the van der Waals' free diameter. They are listed in Table 2. σ_{host} in the present case is $\sigma_{O-O} = 2.529$ Å and $\sigma_{C_n-C_n} = 3.4$ Å for $AlPO_4$-5 and carbon nanotube, respectively. For $AlPO_4$-5, a simple arithmetic average over both narrow and wide regions yielded R. As can be seen from Figure 2b, the minimum in the ethane−host interaction is near the wall of the channel for both of the hosts.

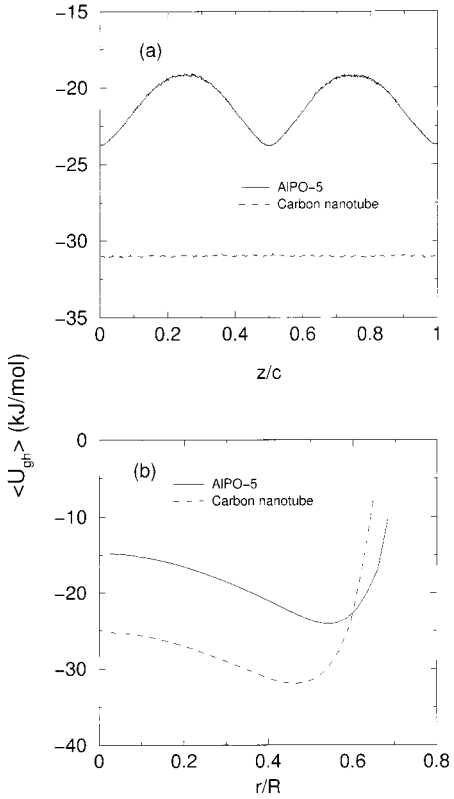

Figure 2. Panel a shows $\langle U_{gh}\rangle$ of ethane as a function of the z coordinate of its center of mass at $T = 200$ K. z is scaled by unit cell length c for $AlPO_4$-5 and by $c = 49.294$ Å for carbon nanotube. Panel b shows $\langle U_{gh}\rangle$ of ethane as a function of r, the perpendicular distance of the center of mass of ethane from the channel axis, at $T = 200$ K. r is scaled by the radius of the respective channel, R.

TABLE 2: Dimension of the Narrowest and the Widest Part of the Channel

	σ_w (Å)	$d_w = \sigma_w - \sigma_{host}$ (Å)	R (Å)
$AlPO_4$-5	10.02	7.49	4.08
	11.37	8.84	
carbon nanotube	10.80	7.4	3.7

TABLE 3: Average Interaction Energy

	ΔH_{ads} (kJ/mol)	$\langle U_{gg}\rangle$ (kJ/mol)	P (kPa)
$AlPO_4$-5	−24.04 (−18.7,[10] −24[11])	−0.2941	3.13
carbon nanotube	−32.66	−0.2620	10.98
bulk ethane		−11.74	

Table 3 lists heat of adsorption ΔH_{ads} values calculated from $\Delta H_{ads} = \langle U_{gh}\rangle - RT$, where R is the gas constant and temperature $T = 200$ K along with the experimental values within parentheses. The experimental ΔH_{ads} value has been determined over the temperature range of 303−473 K for $AlPO_4$-5.[10,11] Table 3 also lists $\langle U_{gg}\rangle$ values, which are much smaller than the corresponding $\langle U_{gh}\rangle$ values. The pressure values as calculated from the virial are also listed in Table 3. It is seen that the pressures are low, which is to be expected from the concentrations (0.2049 mmol/g for $AlPO_4$-5 and 0.26 mmol/g for carbon nanotube).

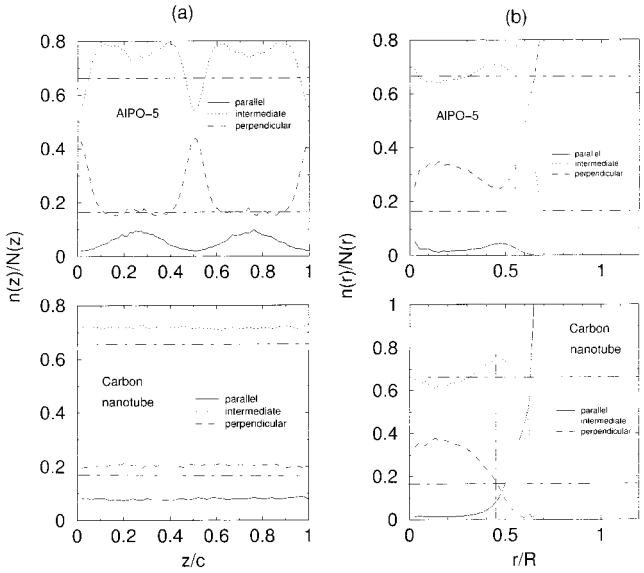

Figure 3. Panel a shows the ratio $n(z)/N(z)$ as a function of position of center of mass of ethane along the channel. $n(z)$ is the number of ethane molecules in a given state of orientation at z, and $N(z)$ is the total number of molecules at z. z is scaled by the unit cell length c for $AlPO_4$-5 and by $c = 49.294$ Å in case of carbon nanotube. Panel b shows the ratio $n(r)/N(r)$ as a function of radial distance of the center of mass of ethane from the channel axis, r. $n(r)$ is the number of ethane molecules in a given state of orientation at r, and $N(r)$ is the total number of molecules at r. r is scaled by the radius of respective channel, R. Also plotted is a line (− - −) parallel to the ordinate indicating the value of r/R at which $\langle U_{gh} \rangle$ is minimum and therefore the total density is a maximum as a function of r. The fraction of molecules in the three orientation intervals for ethane, the orientations of which are randomly distributed, are indicated by lines (− - −) parallel to the abcissa at $^1/_6$ and $^4/_6$ in both panel a and panel b. See text for discussion.

The orientation of ethane can be represented by the angle θ made by the CH_3-CH_3 bond with respect to channel axis. We classify the orientation of ethane into three groups, $\theta < 15°$, $15° < \theta < 75°$, and $\theta > 75°$, which are termed as *parallel*, *intermediate*, and *perpendicular*, respectively. Any given ethane molecule inside a channel has one of these three orientations. Figure 3a shows the ratio, $n(z)/N(z)$, plotted as a function of z. $n(z)$ is the number of ethane molecules lying in one of the above three groups and their center of mass between z and $z + dz$. $N(z)$ is the total number of molecules having their center of mass between z and $z + dz$. From Figure 3a, it is evident that the intermediate orientation is the largest fraction, partly because of its wide range. However, for the purposes of our discussion, it is the other two orientations that are of importance. In carbon nanotube, the perpendicular orientation is populated more than the parallel orientation. In $AlPO_4$-5, the important point to note is that the fraction of ethane molecules with perpendicular orientation is higher in the wider region as compared to that in the narrow region. To understand these, we look at the orientations as a function of r.

Figure 3b shows the ratio $n(r)/N(r)$ plotted as a function of r. $n(r)$ is the number of ethane molecules having one of the three orientations and having their center of mass between r and $r + dr$ from the channel axis, while $N(r)$ is the total number of molecules. In carbon nanotube, near the channel wall, the parallel orientation is populated the most, while in $AlPO_4$-5, the perpendicular orientation is preferred by ethane molecules near the channel wall. Why are there different dependencies in the two channel systems? For this purpose, we show the ratio $n(r)/N(r)$ for different orientations of ethane in narrow and wider parts of the channel in $AlPO_4$-5 (see Figure 4). It can be seen

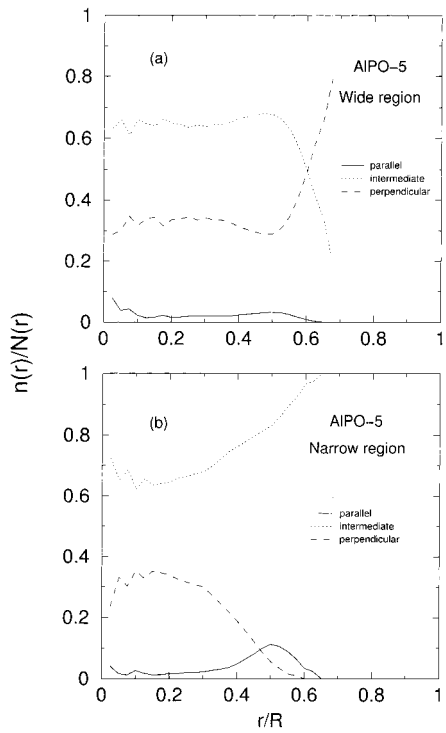

Figure 4. The ratio $n(r)/N(r)$ as a function of radial distance of the center of mass of ethane from the channel axis r in $AlPO_4$-5. $n(r)$ is the number of ethane molecules in a given state of orientation at r, and $N(r)$ is the total number of molecules at r. Panel a represents the wider region of the $AlPO_4$-5 channel; panel b represents the narrow region of the $AlPO_4$-5 channel. r is scaled by the radius of the channel, R.

that the orientational preference in these two parts of the channel is different. The following observations can be made: (a) At large r/R, the preference in the narrow part of the channel is for parallel orientation, while in the wider part, the perpendicular orientation is preferred. The latter is surprising and counter intuitive. (b) At small r, the perpendicular orientation is always preferred over the parallel orientation in both narrow and wider parts of channel.

Also shown in Figure 3 is the fraction of ethane molecules in parallel, intermediate, and perpendicular orientations when the orientations are completely random. In such an instance, the populations will be proportional to the width of the interval (0°−15°, 15°−75°, and 75°−90°), and therefore, the fraction of molecules in each interval are $^1/_6$, $^4/_6$, and $^1/_6$, respectively. It is seen that the population of perpendicular orientations is enhanced in wider regions of $AlPO_4$-5 and in carbon nanotube as compared to the population in random orientation. The population of parallel orientation however is reduced as compared to the random orientations as a function of channel length. The intermediate orientations are lower in the wider region of $AlPO_4$-5 and greater in the narrower regions relative to the random orientations. As a function of r, the populations in both $AlPO_4$-5 and carbon nanotube show significant deviations from the random orientations.

To understand these results, we have looked at the dependence of the guest−host interaction energy as a function of the radial distance within the $AlPO_4$-5 channel in the narrow and wide sections. Figure 5 shows a plot of the variation of U_{gh} with r in narrow and wide parts of the $AlPO_4$-5 channel for perpendicular and parallel orientations. These have been obtained by calculating sorbate−host interaction energy, U_{gh}, for each value of r at narrow and wider cross-sections of the channel under specified

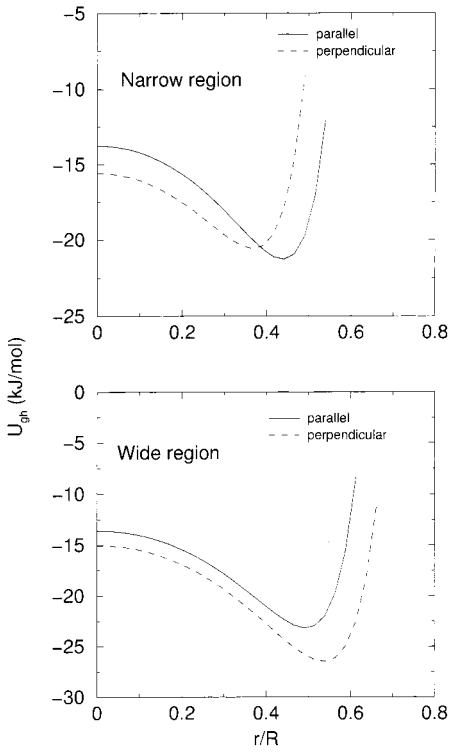

Figure 5. Variation of U_{gh} as a function of radial distance of the center of mass of ethane from the channel axis in narrow and wide parts of the channel for parallel and perpendicular orientations.

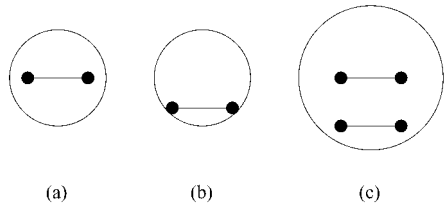

Figure 6. Schematic diagram of ethane inside a channel illustrating (a) why a perpendicular orientation is preferred at small *r* in a narrow channel, (b) why a perpendicular orientation is not accommodated at large *r* in a narrow channel, and (c) why a perpendicular orientation is preferred at any *r* in a wide channel.

orientation ($\theta = 0°$ and 90°). These results are, therefore, not from MD simulation. It is seen that only in narrow parts of the channel the preferential orientation changes from perpendicular at small *r* to parallel at large *r*. These results provide insight into the nature of orientation and therefore diffusion in narrow and wide channel systems. In the wide part of the channel, as can be seen from Figures 3 and 4, perpendicular is the preferred orientation at large *r*. Hence, *reorientation of the molecule does not play an important role in the diffusion within these wider channels.* In wide channels, movement *along and across* the channel can be accomplished *without reorientation* by a large angle. Figure 6 exhibits schematically the overlap that is expected from perpendicular orientation in a narrow channel at large *r* along with those expected within a wide channel. From Figure 4, it is seen that in the *narrow region*, at small *r*, perpendicular is preferred over parallel, while at large *r*, parallel is preferred over perpendicular.

A further analysis to see where the parallel and perpendicular orientations are predominantly located is necessary. For this, we have shown the average radial distance *r*/*R* of the center of mass of the different orientational types from the channel axis as a function of position along the channel *z*. This is shown in Figure 7. In carbon nanotube, parallel orientation of ethane is

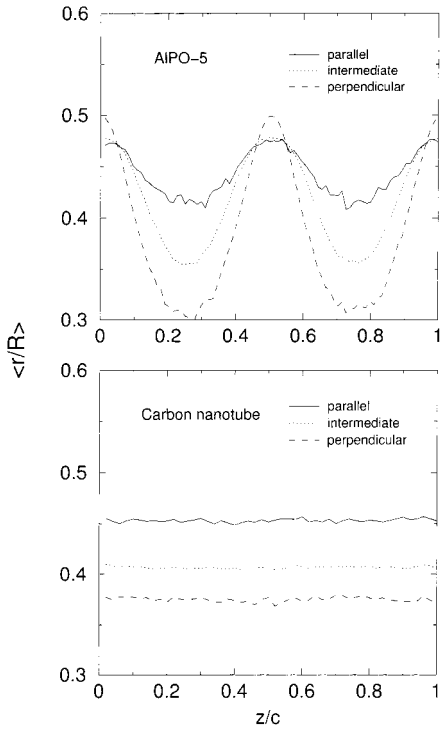

Figure 7. The average radial distance of the center of mass of ethane, $\langle r \rangle$, from the channel axis as a function of the position of the center of mass of ethane along the channel, *z*. $\langle r \rangle$ vs *z* is plotted for parallel, intermediate, and perpendicular orientations of ethane. *r* is scaled by the radius of the respective channel, and *z* is scaled by unit cell length, *c*, in $AlPO_4$-5 and by $c = 49.294$ Å in the case of carbon nanotube.

closest to the channel wall, while perpendicular orientation is closest to the channel axis. In narrow parts of $AlPO_4$-5, parallel orientation is assumed by ethane away from the channel axis, while perpendicular orientation is closer to the channel axis. In wider parts of the channel in $AlPO_4$-5, parallel and intermediate orientations are at the same distance *r* from the channel axis, while perpendicular orientation is slightly closer to the channel wall. These results suggest that the precise orientation of ethane is a function of the distance of the molecular center of mass from the channel axis and the diameter of the channel. In the case of $AlPO_4$-5, the orientation undergoes large changes as a function of *r* as well as *z*.

5.2. Dynamical Properties. *Translational Motion.* Figure 8 shows the mean squared displacement of ethane in $AlPO_4$-5, carbon nanotube, and bulk. $\langle u^2(t) \rangle$ shows linear behavior in $AlPO_4$-5 and bulk liquid. In carbon nanotube, $\langle u^2(t) \rangle$ does not go over to a diffusive regime. For ethane in carbon nanotube, the exponent α in $\langle u^2(t) \rangle \approx t^\alpha$ obtained from the log−log plot is 1.8. This value is closer to the ballistic motion ($\alpha = 2$) than diffusive motion ($\alpha = 1$). Ethane motion along the *z* direction in nanotube, unlike in $AlPO_4$-5, experiences an almost uniform potential energy surface along the channel (see Figure 2a), which leads to nearly free particle-like motion. When this is coupled with nonballistic motion along radial directions, one obtains a value between 1 and 2 for the exponent α. At higher loadings, the motion of ethane can be single-file or diffusive[7] depending on the diameter of the nanotube. In a simulation in which the framework of the carbon nanotube is flexible, the randomness associated with the sorbate motion is expected to increase. This can lead to a lower value of the exponent α. More detailed investigations of motion within carbon nanotube are in progress.

Earlier[5,8] MD and QENS studies of ethane in $AlPO_4$-5 pertain to high loading. The present result that ethane at dilute

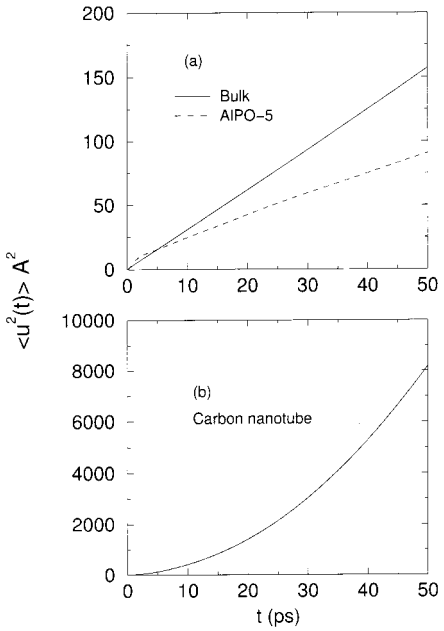

Figure 8. Mean squared displacement of the center of mass of ethane plotted for (a) bulk and $AlPO_4$-5 and (b) carbon nanotube at $T = 200$ K.

TABLE 4: Characteristic Dimensions of the Host Channel

	σ_{gh} (Å)	$2(2^{1/6}\sigma_{gh} + l/2)$ (Å)	γ	$\langle\theta\rangle$ (deg)
$AlPO_4$-5 narrow part	3.152	8.606	0.858	~48
$AlPO_4$-5 wider part		8.606	0.757	~64
carbon nanotube	3.588	9.585	0.887	~50

TABLE 5: Self-Diffusion Coefficient

	D^t, (10^{-8} m^2/s)	density, ρ (g/cm^{-3})
$AlPO_4$-5	0.337	0.038
bulk ethane	0.525	0.544

concentration shows simple diffusive behavior is in agreement with those of Demontis et al.[5] at higher loading.

The self-diffusion coefficient for ethane in bulk and in $AlPO_4$-5 is obtained from Einstein's relation,

$$D^t = \frac{\langle r^2 \rangle}{6t} \tag{2}$$

and is listed in Table 5. These values have been obtained from the slope of the straight line fitted to data in the interval 10−40 ps. The error in D^t for ethane in $AlPO_4$-5 and in bulk is 2.4% and 2%, respectively.

The velocity autocorrelation function (VACF) of ethane in the space-fixed frame is shown in Figure 9a for $AlPO_4$-5, carbon nanotube, and bulk. It is seen that motion in $AlPO_4$-5 along the channel (z direction) is more facile than that in the other two directions though all exhibit negative correlation. A negative minima is seen around $t = 0.5$ ps for z component in $AlPO_4$-5. This is due to the narrow part of the channel at $z/c = 0.25$ and 0.75. Within carbon nanotube, it is seen that the VACF of the z component of the velocity does not decay leading to nondiffusive motion. For motion in bulk, it is seen that the correlations persist over longer times despite its high density. In $AlPO_4$-5 and carbon nanotube, the oscillations around $t = 1$ ps along the x and y directions are due to the confinement.

VACF of x, y, and z components in the body-fixed frame of reference (the z axis of which coincides with the molecular axis) is shown in Figure 9b. In bulk ethane, motion along the z axis

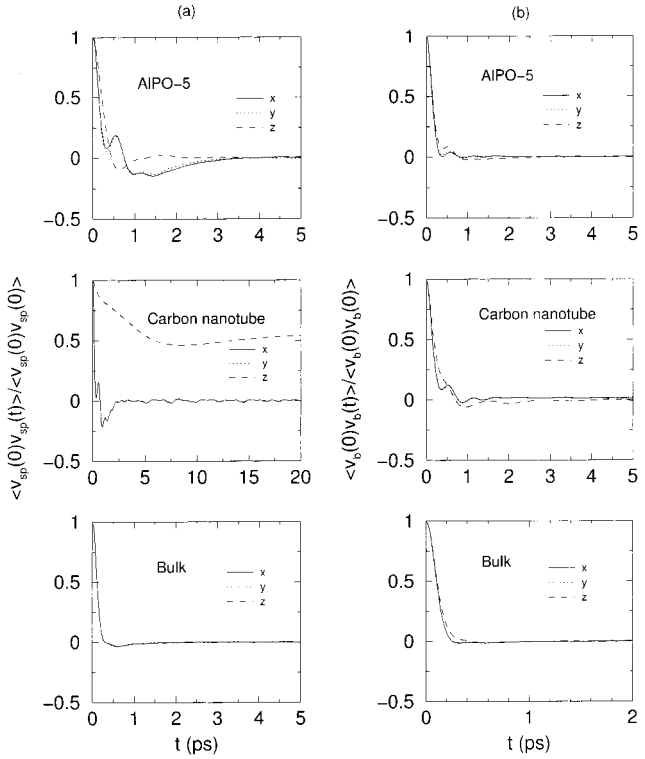

Figure 9. VACF plotted for the center of mass of ethane in (a) a space-fixed frame of reference for ethane in $AlPO_4$-5, carbon nanotube, and bulk at $T = 200$ K and (b) a body-fixed frame of reference (z-axis coincides with the molecular axis) for ethane in $AlPO_4$-5, carbon nanotube, and bulk at $T = 200$ K.

is seen to be relatively more facile than that in the other two directions. Note that the ratio of molecular dimensions perpendicular and parallel to the C_2 axis is 5.3 Å/3.775 Å ≈ 1.4. In confined systems, all of the components of VACF show oscillations suggesting the presence of obstructions. Note that in both $AlPO_4$-5 and carbon nanotube the angle θ is far from zero (see Table 4). As a result, motion along all three directions is more or less identical.

Rotational Motion. The angular velocity autocorrelation function (AVACF) in the body-fixed frame is shown in Figure 10a. It is seen that rotation around the x and y directions shows more oscillations in carbon nanotube as compared to those in $AlPO_4$-5. This is again because a predominant fraction of ethane is present in the wider part of the $AlPO_4$-5 channel. Therefore, the AVACF in $AlPO_4$-5 shows less oscillations suggesting lower hindrance to rotation of ethane than that in carbon nanotube. The AVACF shows smooth decay in bulk. It is to be noted that the oscillations in AVACF in carbon nanotube and $AlPO_4$-5 occur at or around $t = 1$ ps. Rotational diffusivity is calculated from

$$D_i^r = \int_0^\infty \langle \omega_i(0)\omega_i(t) \rangle \, \mathrm{d}t \tag{3}$$

where $i = x, y$. Integration of the AVACF is performed up to 12 ps. The rotational diffusivity values are listed in Table 6. First, we note that confined ethane has a higher value of D^r than that in bulk. From the tabulated values, it is clear that ethane has a rotational diffusivity in carbon nanotube about 3−4 times greater than that in $AlPO_4$-5. However, it is surprising that ethane in $AlPO_4$-5 has lower value of D^r than ethane in carbon nanotube. As already mentioned, the wider part of the channel of $AlPO_4$-5 (where ethane resides most of the time) has a larger

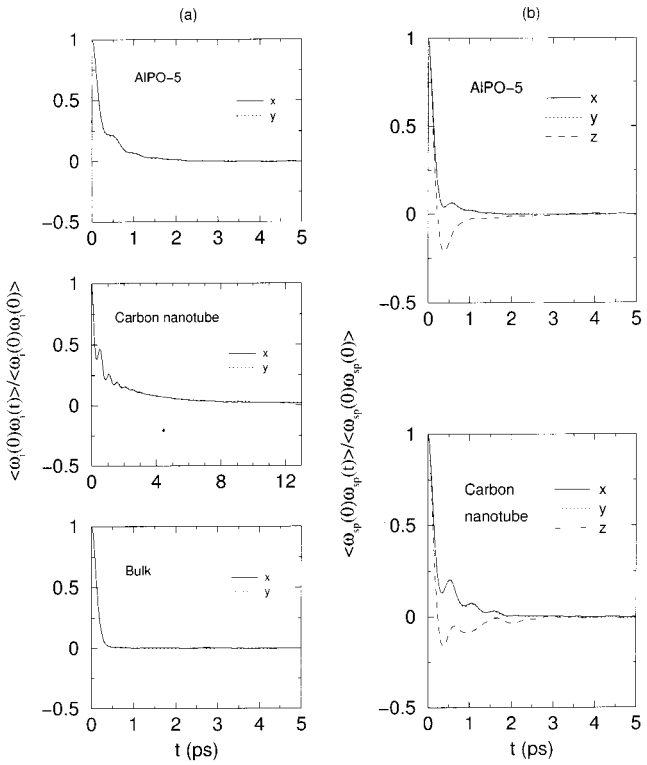

Figure 10. Angular VACF plotted (a) in a body-fixed frame of reference for ethane in $AlPO_4$-5, carbon nanotube, and bulk at $T = 200$ K and (b) in a space-fixed frame of reference for $AlPO_4$-5 and carbon nanotube at $T = 200$ K.

TABLE 6: Rotational Diffusivity of Ethane

	D_x^r (ps^{-1})	D_y^r (ps^{-1})
$AlPO_4$-5	2.85	2.87
carbon nanotube	10.76	11.00
bulk ethane	1.39	1.38

diameter than carbon nanotube. The present result seems to suggest that D^r *is higher in channels of smaller diameter*.

AVACFs calculated in the space-fixed frame are shown Figure 10b. An oscillatory pattern similar to that observed in the body-fixed frame is seen for *x* and *y* components. Because the angle θ is nonzero, it is to be expected that the *z* component is nonzero and finite. However, what is surprising is that the *z* component makes a pronounced foray into the negative region, while *x* and *y* components do not exhibit similar trends. This is true for both $AlPO_4$-5 and carbon nanotube. This can be understood if we look at both the translational motion (as indicated by VACFs) and rotational motion simultaneously. Free rotation around the channel axis (*z* axis) would only be possible if the center of mass of ethane is close to the channel center and not otherwise. From the *x* or *y* component of VACF in the space-fixed frame (Figure 9a), it is seen that the velocity of the center of mass is nearly reversed in about 0.4 ps. During this time, ethane would have traversed a distance that is comparable to the radius of the channel. This is also apparent from the mean squared displacement shown in Figure 8. As a result, one of the two CH_3 groups would collide with the channel wall (because $\langle\theta\rangle$ is nonzero), and this leads to a complete reversal of the *z* component of angular velocity. Contrast this with rotation around the *x* or *y* directions in the space-fixed frame, which will be only affected by the motion of the ethane along the *z* axis where no collision with the wall takes place, and therefore, one does not see any reversal of the angular velocity but only oscillations. The oscillations are larger in amplitude

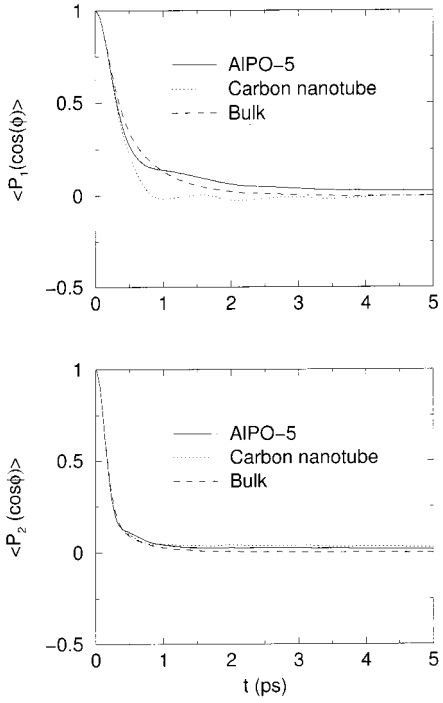

Figure 11. Reorientational correlation function, $\langle P_l(\cos(\phi))\rangle$, plotted for $l = 1, 2$ for ethane in $AlPO_4$-5, carbon nanotube, and bulk at $T = 200$ K.

TABLE 7: Reorientational Correlation Time of Ethane

	τ_1 (ps)	τ_2 (ps)	τ_2/τ_1
$AlPO_4$-5	0.82	0.64	0.78
carbon nanotube	0.29	0.97	3.34
bulk ethane	0.49	0.25	0.51

in the case of carbon nanotube as a consequence of its narrow diameter when compared with the wider part of $AlPO_4$-5 channel where, as already noted, ethane resides most of the time.

Figure 11 shows the reorientational correlation function, $P_l(\cos\phi(t))$, plotted for $l = 1, 2$. $\phi(t)$ is the angle between the direction of the unit vector along the CH_3-CH_3 bond at some initial time $t = 0$ and time *t*. From the plot, it can be seen that after the initial inertial decay of correlations ($t < 0.5$ ps) the long time decay of reorientational correlations in bulk is different from that in confinement. This can be seen from reorientational correlation time calculated as follows:

$$\tau_l = \int_0^{t_{max}} \langle P_l(\cos\phi(t))\rangle \, dt \qquad (4)$$

for $l = 1, 2$. Integration is performed up to $t_{max} = 30$ ps for $AlPO_4$-5 and carbon nanotube and bulk ethane. These values are listed in Table 7. The Debye model predicts $\tau_2/\tau_1 = {}^1/_3$ (ref 23). As Table 7 indicates, reorientation of ethane in bulk is close to the Debye model prediction. In the case of $AlPO_4$-5 and carbon nanotube, however, the ratio deviates significantly from the Debye model. This is due to a large increase in τ_2 in confinement as compared to the bulk value. τ_1 does not increase significantly in confinement as compared to τ_2.

6. Conclusion

The present study shows that the orientation of ethane is a function of *z*, the position of the center of mass along the channel, and the channel radius *R* in one-dimensional channels of $AlPO_4$-5 and carbon nanotube. The crossover from parallel to perpendicular orientation during the motion of ethane along

TABLE 8: Orientation of Ethane Inside $AlPO_4$-5 and Carbon Nanotube

	near the channel axis	near the channel wall
$AlPO_4$-5		
wide part	⊥	⊥
narrow part	⊥	∥
carbon nanotube	⊥	∥

the $AlPO_4$-5 channel when the center of mass is close to the wall is due to the undulations in the channel diameter and crossover in the guest−host potential energy function (see Figures 4 and 5). Principal results regarding orientation of ethane inside $AlPO_4$-5 and carbon nanotube are summarized in Table 8. These results suggest that molecular reorientation of linear molecules such as ethane does not influence strongly the translational mobility of ethane both along and across the wider part of the $AlPO_4$-5. This is, however, not the case in the narrow part of $AlPO_4$-5 channel as well as carbon nanotube where motion across the channel requires ethane to change its orientation from perpendicular to parallel.

Ethane at the dilute concentrations investigated here shows diffusive motion inside $AlPO_4$-5. This is in agreement with experimental and MD studies. A recent MD study by Demontis et al.[5] has reported subdiffusive behavior at a loading of one ethane per unit cell. Superdiffusive behavior, $u^2(t) \approx t^\alpha$, $\alpha = 1.8$, is seen for ethane in carbon nanotube at dilute concentrations. Because ethane molecules may not be able to overtake each other within the channels of carbon nanotube, it is likely that at higher loading they may exhibit a single-file behavior where $u^2(t) \propto t^\alpha$, where $\alpha = 0.5$.

Surprisingly, the AVACF of the component along the channel axis shows a pronounced negative minimum. This is shown to be due to the collision of the methyl group with the channel wall during the translation of the center of mass of ethane. The evidence for this is seen in the mean squared displacement plot.

The rotational motion around the long axis of the channel is strongly influenced by the restrictions along directions perpendicular to this long channel axis. One can expect that this influence will be greater when the molecule is longer. Confinement causes reorientational correlations to persist for longer times than those in bulk. This leads to significant deviation of the ratio τ_2/τ_1 from the $^1/_3$ predicted by the Debye model.

Apart from the united atom model as used for ethane in present study, ethane molecule can also be modeled with a separate site for each of the C and H atoms and with inclusion of torsional motion. In such a fully atomistic model of ethane, dynamical properties, especially those associated with rotational dynamics, are likely to be altered. The barrier for torsional motion is large (~3 kcal/mol). Hence, it is unlikely that torsional motion will play an important role at the temperature and the density of ethane used in present study. The moment of inertia will be slightly larger for an eight-site model of ethane, as a consequence of which the rotational motion may be slower. Flexibility of hosts would lead to increased randomness in the sorbate motion, which could cause the motion to become more diffusive.

Acknowledgment. Financial support from the Department of Science and Technology, New Delhi (Project No. SP/S1/H-12/99), and CSIR, New Delhi, is gratefully acknowledged.

References and Notes

(1) Kärger, J.; Ruthven, D. M. *Diffusion in Zeolites and Other Microporous Solids*; John Wiley: New York, 1992.
(2) Bates, S. P.; van Santen, R. A. *Adv. Catal.* **1997**, *42*, 1.
(3) Clark, L. A.; Ye, G. T.; Gupta, A.; Hall, L. L.; Snurr, R. Q. *J. Chem. Phys.* **1999**, *111*, 1209.
(4) Gergidis, L. N.; Theodorou, D. N.; Jobic, H. *J. Phys. Chem. B* **2000**, *104*, 5541.
(5) Demontis, P.; Gonzalez, J. G.; Suffritti, G. B.; Tilocca, A. *J. Am. Chem. Soc.* **2001**, *123*, 5069.
(6) Sholl, D. S. *Chem. Eng. J.* **1999**, *74*, 25.
(7) Mao, Z.; Sinnott, S. B. *J. Phys. Chem. B* **2000**, *104*, 4618.
(8) Jobic, H.; Hahn, K.; Kärger, J.; Bée, M.; Tuel, A.; Noack, M.; Girnus, I.; Gordon, J. K. *J. Phys. Chem. B* **1997**, *101*, 5834.
(9) Gupta, V.; Nivarthi, S. S.; McCormick, A. V.; Davis, H. T. *Chem. Phys. Lett.* **1995**, *247*, 596.
(10) Choudhary, V. R.; Mayadevi, S. *Sep. Sci. Technol.* **1993**, *28*, 2197.
(11) Jänchen, J.; Stach, H.; Uytterhoeven, L.; Mortier, W. J. *J. Phys. Chem.* **1996**, *100*, 12489.
(12) Maris, T.; Vlugt, T. J. H.; Smit, B. *J. Phys. Chem. B* **1998**, *102*, 7183.
(13) Richardson, J. W., Jr.; Pluth, J. J.; Smith, J. V. *Acta Crystallogr.* **1987**, *C43*, 1469.
(14) Ayappa, K. G. *Langmuir* **1998**, *14*, 880.
(15) Zhang, F. *J. Chem. Phys.* **1999**, *111*, 9082.
(16) Jorgensen, W. L.; Madura, J. D.; Swenson, C. J. *J. Am. Chem. Soc.* **1984**, *106*, 6638.
(17) Bandyopadhyay, S.; Yashonath, S. *J. Phys. Chem.* **1995**, *99*, 4286.
(18) Bhide, S. Y.; Yashonath, S. *J. Chem. Phys.* **2002**, *116*, 2175.
(19) Steele, W. A. *Surf. Sci.* **1973**, *36*, 317.
(20) Allen, M. P.; Tildesley, D. J. *Computer Simulation of Liquids*; Clarendon Press: Oxford, U.K., 1987.
(21) Bhide, S. Y.; Yashonath, S. *J. Phys. Chem. B* **2000**, *104*, 11977.
(22) Derouane, E. G.; André, J. M.; Lucas, A. L. *J. Catal.* **1988**, *110*, 58.
(23) Berne, B. J.; Pecora, R. *Dynamic Light Scattering*; John Wiley: New York, 1976.